Journal of Optics

PAPER

Optical analogy of gravitational collapse and quantum tunneling of the event horizon

IOP Publishing Journal of Optics
J. Opt. 22 (2020) 035605 (8pp) https://doi.org/10.1088/2040-8986/ab6f49

Optical analogy of gravitational collapse and quantum tunneling of the event horizon

Jingming Chen[1,4], **Run-Qiu Yang**[2,3], **Shining Zhu**[1] **and Hui Liu**[1,4]

[1] National Laboratory of Solid State Microstructures and School of Physics, Collaborative Innovation Center of Advanced Microstructures, Nanjing University, Nanjing, Jiangsu 210093, People's Republic of China
[2] Quantum Universe Center, Korea Institute for Advanced Study, Seoul 130-722, Republic of Korea
[3] Center for Joint Quantum Studies, School of Science, Tianjin University, Yaguan Road 135, Jinnan District, 300350 Tianjin, People's Republic of China

E-mail: chenjingming24@163.com and liuhui@nju.edu.cn

Received 27 June 2019, revised 14 January 2020
Accepted for publication 23 January 2020
Published 12 February 2020

Abstract

We present an optical method to realize the analogy of gravitational collapse by using the gradient of the refractive index system and the spacetime embedding diagram. We observe an analogy of Hawking radiation after the horizon is formed, for which the corresponding effective temperature is obtained via the transmission spectrum. We find that the effective temperature is proportional to the surface gravity, which is similar to the case in real black holes.

Keywords: gravitational collapse, Hawking radiation, embedding diagram, projected refractive index, analogue gravity

1. Introduction

Research on black holes has attracted attention for a long time. In particular, after the successful detection of a black hole's gravitational wave in 2015 [1] and the first picture of black hole taken by the horizon telescope in 2019 [2], scientists now believe that black holes exist widely in our universe. We now acknowledge that a black hole is formed by the gravitational collapse of a massive star (to form a black hole the mass of this star should be larger than Oppenheimer's limit, i.e. $M > 3.2M_{\mathrm{sun}}$). So research about this dynamic process is crucial to understand the formation of black holes. In the last century, many outstanding theoretical physicists such as Hawking and Penrose have analyzed this dynamic process theoretically [3–5]. In 2000, Sonego *et al* theoretically studied the optical geometry in the gravitational collapse of spacetime and described this process semi-quantitatively with a 2D surface [6]. Additionally, in 2019, Baumgarte *et al* numerically investigated the threshold of black-hole formation in the axisymmetric gravitational collapse of electromagnetic waves and discussed implications for the critical collapse of vacuum gravitational waves [7]. Nevertheless, experimental simulations and astronomical observations of gravitational collapse are still very limited.

At present, only very few of the classical properties of black holes can be observed. Observation of the quantum properties of black holes is quite difficult. Many quantum properties of black holes are closely related to the event horizon, so research into the event horizon is crucial for making progress in the quantum properties of black holes. The most famous research that involves the horizon is known as Hawking radiation. Though we have not observed Hawking radiation of a black hole so far, theorists proposed that the process of Hawking radiation can be simulated by analogy to certain experimental systems. In 1981, Unruh presented an analogy of Hawking radiation in an acoustic black hole system [8]. He found that when the fluid exceeds the speed of sound, the sound waves are trapped in a supersonic region, and Hawking radiation of the phonon exists near the sonic horizon. In 2009, Steinhauer and his collaborators first obtained a stable supersonic Bose–Einstein condensate (BEC) fluid and calculated the Hawking temperature at an order of magnitude of 0.1 nK [9]. In their latest research, they observed that the spectrum of Hawking radiation agrees well with a thermal spectrum in an improved BEC system, in analogy with a real black hole [10]. In 2008, Philbin *et al* used nonlinear optical fibers to simulate the event horizon of a

[4] Authors to whom any correspondence should be addressed.

white hole and observed the blue shift of light near the horizon [11]. In 2019, Drori *et al* observed stimulated Hawking radiation based on the same nonlinear fiber systems [12]. Although these analogous experimental systems with some approximations can simulate certain effects of curved spacetime, they still cannot accurately correspond to real curved spacetime.

In the past 20 years, developments in material fabrication and measurement techniques have encouraged us to make numerous attempts about analogue curved spacetime such as black holes [13–17], wormholes [18, 19], Einstein ring [20], De-Sitter space [21], cosmological inflation, redshift [22], cosmic string and topological defects [23]. In the most recent decade, a curved waveguide based on the surface of the embedding diagram of the metric has become another new optical structure to mimic curved space and the effect of general relativity [24–27]. At present, research on a curved waveguide that simulates curved spacetime still remains within the classical characteristics of the gravitational field. So it is quite worthwhile to try to simulate the quantum characteristics with a curved waveguide.

In order to describe the casual structure of a black hole, Penrose proposed a widely accepted schematic method called Penrose diagrams [3–5]. The Penrose diagram is a good tool to exhibit global causal structure; it is not suitable to present the curvature of spacetime. There is also an alternative diagrammatic method named 'embedding diagram' in the study of black holes, which is widely used to visualize the curvature of spacetime. In this paper, we make a step in describing the process of gravitational collapse of a star and the formation of horizon, using a one-dimensional embedding diagram [28–30] and the gradient of refractive index systems. We will show numerically that our model can present an analogy of Hawking radiation after the horizon is formed, from which the Hawking temperature is obtained directly from the transmission rate. We found numerical results can match quite well the theoretical predictions of Hawking radiation.

This paper is organized as follows. In section 2, we present our optical model of gravitational collapse in one-dimension gradient of the refractive index. In section 3, we give an optical analogy of the Hawking radiation index system and compare the effective temperature with the Hawking temperature formula. Then we conclude in section 4.

2. Analogy of gravitational collapse using the gradient of the refractive index

Let us first recall the basic description of gravitational collapse. One picture of the process of gravitational collapse can be understood as follows: a beam of light is incident on a collapsing star, crosses the center of star, then 'reflects' and propagates outwards to infinity. Specifically, if we assume that when incident light arrives at star at time $t = t_0$, the event horizon has just formed, and the light is trapped into the horizon. After that the star collapses rapidly to form a black hole. All incident light beams later than the initial time ($t > t_0$) will be totally absorbed into the central singularity by the strong curvature of spacetime and cannot get outwards anymore.

First, we assume that the exterior region is in vacuum. Due to the spherical symmetry, the spacetime metric of the exterior region is given by Schwarzschild solution (in this paper, we take $G = c = \hbar = k_B = 1$) given by equation (1):

$$ds^2 = -\left(1 - \frac{2M}{r}\right)dt^2 + \left(1 - \frac{2M}{r}\right)^{-1}dr^2 + r^2(d\theta^2 + \sin^2\theta d\varphi^2),\ R(t) \leqslant r < \infty, \tag{1}$$

where $R(t)$ is the radial coordinate of the star, which evolves with time t. M is the mass of central star. The surface gravity κ, which describes the gravitational strength measured by observers at spatial infinity, depends on the mass with equation (2):

$$\kappa = \frac{1}{4M}. \tag{2}$$

The interior geometry of star is much more complicated in that it depends on the detailed structure and interaction of matter within the star. We need to add several assumptions to simplify this situation. First, we suppose that the spherically symmetric star consists of a perfect fluid and ignore all thermodynamic effects, which was discussed in detail by Oppenheimer and Volkoff in 1938 [31, 32]. Starting with the Tolman–Oppenheimer–Volkoff equation, we can get the interior metric from equation (3):

$$\begin{aligned} ds^2 &= -e^{2A(r)}dt^2 + \left(1 - \frac{2m(r)}{r}\right)^{-1}dr^2 \\ &\quad + r^2(d\theta^2 + \sin^2\theta d\varphi^2),\ 0 < r < R(t) \\ A(r) &= -\int_r^\infty \frac{2}{r'^2}(m(r') + 4\pi r'^3 P(r')) \\ &\quad \times \left(1 - \frac{2m(r')}{r'}\right)^{-1}dr', \end{aligned} \tag{3}$$

where $m(r') = \int_0^r 4\pi\rho r'^2 dr'$, and $P(r')$ and ρ are, respectively, the pressure and density inside the star.

Second, we assume that star has uniform density and zero pressure that is usually called a 'ball of dust.' In the boundary between the interior and exterior regions, the metric should be continuous. So we have the boundary conditions given by equation (4):

$$m(R) = M, \quad e^{2A(R)} = 1 - \frac{2M}{R}. \tag{4}$$

Based on the above assumptions, we can rewrite the interior metric as equation (5):

$$ds^2 = -e^{2A(r)}dt^2 + \left(1 - \frac{2M}{R(t)^3}r^2\right)^{-1}dr^2 + r^2(d\theta^2 + \sin^2\theta d\varphi^2),\ 0 < r < R(t). \tag{5}$$

It is very similar to the Friedmann–Lemaitre–Robertson–Walker (FLRW) metric with positive space curvature as illustrated in figure 1.

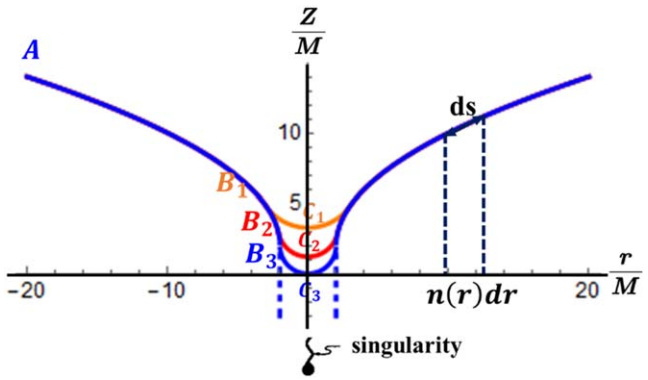

Figure 1. Embedding diagrams: embedding curves described by equation (10) with $R = 3M$ (in orange), $R = 2.1M$ (in red) and $R = 2M$ (in blue); the dashed line in blue represents the event horizon, which keeps going down forever. Black dashed line is a schematic diagram of the projected refractive index of 1D curve mentioned later.

Now let us introduce embedding diagrams. They are useful and effective tools that present hidden spatial curvature information of curved space [28–30]. An arbitrary static spherically symmetric metric can be written in the form given by equation (6):

$$ds^2 = g_{tt}dt^2 + g_{rr}dr^2 + r^2(d\theta^2 + \sin^2\theta d\varphi^2). \tag{6}$$

We focus only on the spacetime at a particular moment t and the equatorial plane, which leads to $dt = 0$ and $\theta = \frac{\pi}{2}$. Then metric of equation (6) degrades into 2D form as equation (7):

$$ds^2 = g_{rr}dr^2 + r^2d\varphi^2. \tag{7}$$

We embed the two-dimensional space of equation (7) into a three-dimensional Euclidean space with equivalence of line elements given by equation (8):

$$g_{rr}dr^2 + r^2d\varphi^2 = dZ^2 + dr^2 + r^2d\varphi^2, \tag{8}$$

where the right side is the line element expressed in cylindrical coordinates (r, φ, Z). Then we can derive the embedding diagram equation as equation (9):

$$\frac{dZ}{dr} = \sqrt{g_{rr} - 1}, \tag{9}$$

which reveals a fact that the function of the embedding diagram is uniquely determined by the spatial components g_{rr} of the spacetime metric.

Based on this model, we can derive the one-dimensional smooth curves of embedding of metrics of equations (1)–(5) as given by equation (10):

$$\begin{aligned} Z_{in} &= -\sqrt{\frac{1}{2M}R^3 - r^2} + \sqrt{\frac{1}{2M}R^3 - R^2} \\ &\quad + \sqrt{8M(R-2M)} + C \qquad 0 < r < R(t) \\ Z_{out} &= \sqrt{8M(r-2M)} + C \qquad R(t) < r < \infty, \end{aligned} \tag{10}$$

where C is the integration constant. In this paper, we set $C = 2$ just for simplicity.

As depicted in figure 1, three curves with different colors and notations describe the dynamic process of collapse, where B_n ($n = 1, 2, 3$ correspond to $R = 3M, 2.1M, 2M$, respectively are the positions of the star's edge. Curves AB_n are diagrams of the exterior part at different times, and curves B_nC_n are the interior part. It is noted that the embedding diagram Z_{out} of equation (10) is uniquely determined by the mass of the central star M, and the mass is supposed to be invariable throughout the whole process. So the shape of curves AB_n does not change, extending just to inside the star's edge B_n. While the inner curves shrink and gradually bulge out to B_3C_3, and eventually reaching point B_3, corresponding to the gravitational radius, the whole star collapses in an inexorable and unstoppable way to form a black hole. This means the exterior curve like the blue dashed line goes down forever, and the inner star shrinks sharply to a point with infinite density, called the central singularity.

What needs to be pointed out is that we cannot depict the interior part of black hole because embedding diagram equation (10) is not analytic in that region ($r < 2M$) in the real number field with coordinates (Z, r).

We can regard a one-dimensional curve with constant refractive index as a one-dimensional gradient of the refraction index via the equivalence of the optical path. As the black dashed lines in figure 1 demonstrate, the light ray is confined to propagating along the blue line with constant refractive index $n_0 = 1$, and the corresponding optical path element is $d\sigma = n_0 ds = n_0\sqrt{1 + \left(\frac{dZ}{dr}\right)^2}dr$. For light rays propagating along the r-axis with the gradient of the refractive index $n(r)$, the optical path element is $d\sigma = n(r)dr$.

We get a projected refractive index from the comparison of corresponding path elements using equation (11):

$$n(r) = \sqrt{1 + \left(\frac{dZ}{dr}\right)^2}. \tag{11}$$

This equation expresses the one-dimension refractive index with relevant geometric curvature of curve.

Then we derive the projected index of equation (10) from equation (12):

$$\begin{aligned} n_{in} &= \sqrt{1 + \frac{r^2}{\frac{1}{2M}R^3 - r^2}} \\ n_{out} &= \sqrt{\frac{r}{r-2M}}. \end{aligned} \tag{12}$$

Light propagates in a vacuum or a medium and can be described by the Maxwell equations, and the material equation $n = \sqrt{\varepsilon_r}$. With some simple vector analysis and transformations we can derive standard Helmholtz equation (13):

$$\nabla^2\varphi(x, y, z) + [nk_0]^2\varphi(x, y, z) = 0. \tag{13}$$

This equation is only effective for an isotropic homogeneous medium, n is the effective refractive index of the medium, k_0 is the wave vector in a vacuum, and φ is the electric or magnetic field component. The Helmholtz equation in 1D situation can be expressed as equation (14):

$$\frac{d^2\varphi(x)}{dx^2} + [nk_0]^2\varphi(x) = 0. \tag{14}$$

Furthermore, if the medium is inhomogeneous with a gradient in the refractive index in the direction of propagation,

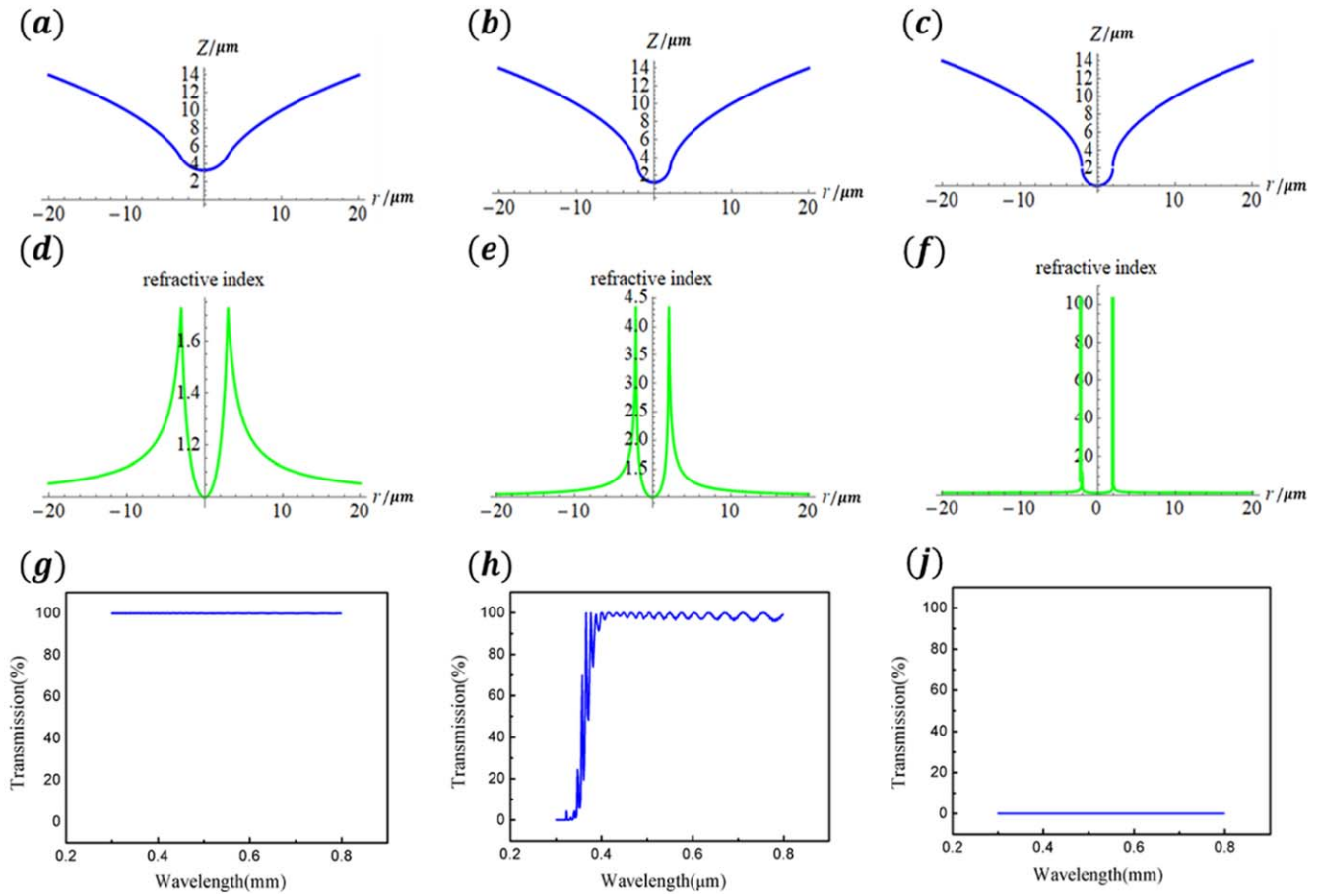

Figure 2. Projected refractive indexes and measurement of transmission spectrum. (a)–(c) Embedding curves with $R = 3$ μm, 2.1 μm and 2.000 02 μm, respectively. (d)–(f) The corresponding projected refractive index. (g)–(i) The corresponding transmission spectrum.

equation (14) should be corrected to (details are shown in appendix A) equation (15):

$$\frac{d^2\varphi(x)}{dx^2} + [n(x)k_0]^2\varphi(x) = 0. \tag{15}$$

Here $n(x)$ is given by equation (12) by substituting x for r. It is noted that this differential equation holds this form only in one dimension and can be solved numerically.

The three corresponding projected refractive indexes of curves depicted in figure 1 are shown in figure 2. It is clear that the corresponding index of the stellar surface increases with the decrement of radius and eventually approaches infinity. In optical systems, the velocity of light falls to zero when it propagates to the region with an infinite refractive index. This feature of light with null speed is very similar to event horizon. In this paper, we intend to use the location of infinite refractive index to simulate the horizon of a black hole.

We stipulate that a plane wave propagates in a refractive index distribution like that of equation (12) with gravitational radius $r_g = 2M = 2$ μm and different R via the finite difference time domain method (FDTD Solutions) and conduct simulations. We establish the distribution of refractive index on a plane waveguide with 100 μm length (the indexes at both ends can be regarded as uniform and equal to one) and 8 μm width in the x and y directions, respectively. A beam of a plane wave with wavelengths ranging from 0.3 to 0.8 μm and unit amplitude is incident from the start point ($x = -50$ μm). The transmission spectra are measured at the end of the waveguide ($x = 50$ μm). We physically explain the transmission spectrum in figures 2(g)–(i) as the region between two peaks of the refractive index, such as second line in figure 2, which is equivalent to an optical potential barrier. As in figure 2(d), the peak of the index is not large; the effective wavelengths of light at this point are comparable to the scale of barrier, so all light transmits as diffraction, leading to figure 2(g). With the increment of peak index light with short effective wavelengths at that point will be blocked by the optical barrier, while long wavelengths light can still transmit from the barrier which leads to the transmission spectrum in figure 2(g). Of course when the peak index is so large that it can be treated as infinite, all effective wavelengths of light are compressed to zero, which means no signals can transmit as shown in figure 2(i). Meanwhile, we obtain a scatter diagram for the transmission of monochromatic plane wave with 0.633 μm wavelength and a star of radius R in figure 3(a). It is obvious that transmissions of the wave sharply decay to almost zero as the radius of star approaches $2M$, which is the location of horizon.

3. Optical analogy of Hawking radiation as tunneling

In the above section, we found that the transmission rate will decay rapidly with respect to the energy of the beam when the

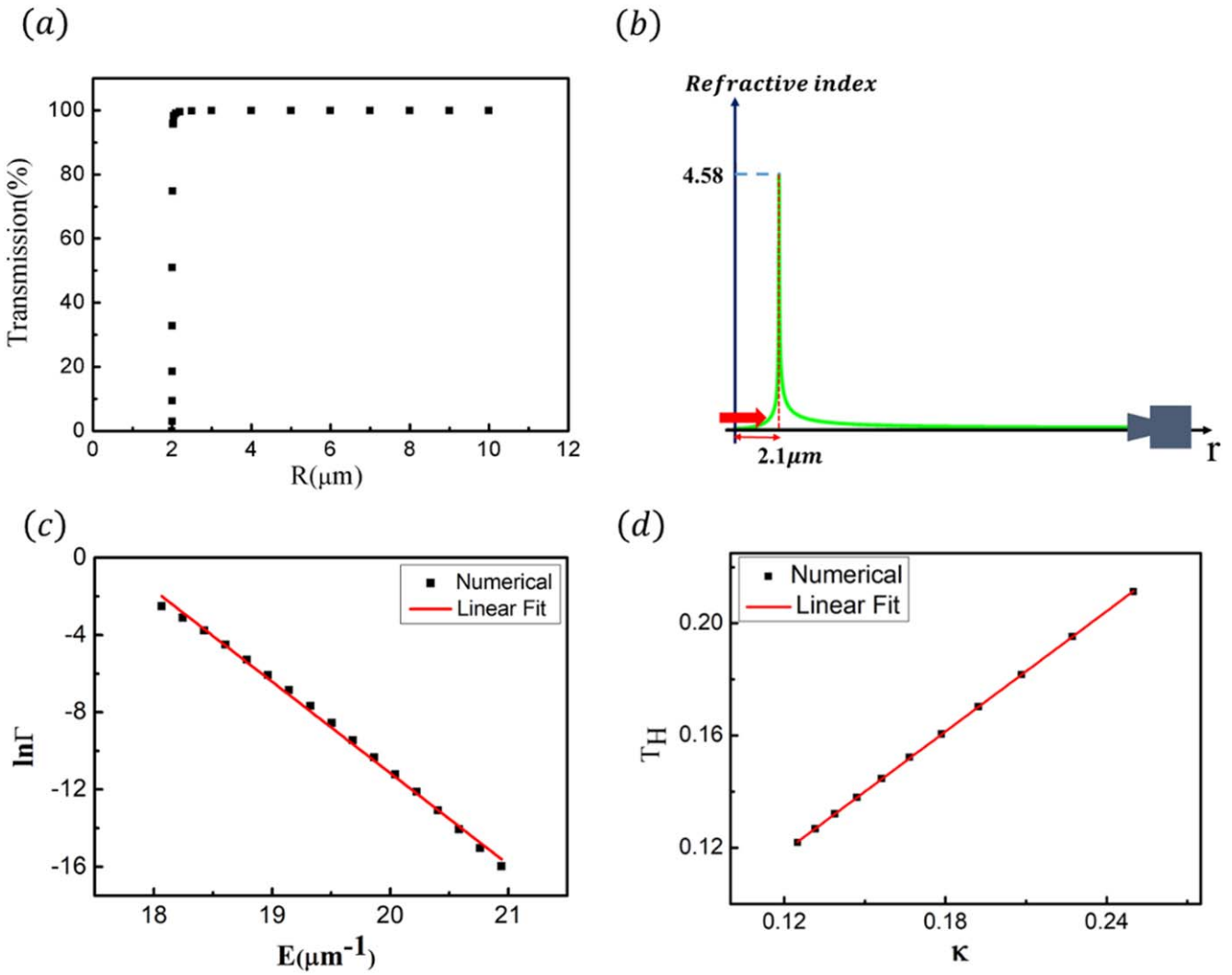

Figure 3. (a) Transmission of plane wave with 633 nm wavelength travels in gradient index like equation (12) with different R and $M = 1$ μm. (b) Schematic diagram of plane waveguide and inner index distribution. (c) Numerical simulation of transmission spectrum of gradient index in equation (12) with $R = 2.1$ μm, $M = 1$ μm and linear fitting of E and $ln\Gamma$. (d) Corresponding Hawking temperature of different black holes with different M and linear fitting with surface gravity κ.

event horizon is almost formed. In this section, we will show that these phenomena are just analogous to Hawking radiation of a black hole formed by collapsed stars.

In 1974, Hawking examined the quantum effects of a collapsing star, which is about to form a black hole. He used a Bogoliubov transformation and found black holes were radiating energy as if they were a blackbody of temperature $T \propto \kappa$ [33, 34]. From aspects of classical and quantum fields, one explanation of Hawking radiation is explained as a pair of particle-antiparticles is created outside the horizon, then the anti-particle with negative energy will fall into black hole, and the particle with positive energy will escape to infinity.

Once inside the black hole, the physical time direction is along -r, so the antiparticle (negative energy) falls into black hole and 'goes forward in time.' In the Feynman path integral formulism, it can be treated as an anti-antiparticle, i.e. particle, 'going backward in time,' actually moving towards the horizon. This process and the pair creation are just virtual processes. The only materialized phenomena is that the black hole reduces its mass, and the outside has a new particle (positive energy). Thus, there is an equivalent picture: a positive energy particle inside the black hole moves towards the horizon (this is a virtual process and is not observable, and so does not valid causality) and succeeds tunneling to the outside of horizon and is seen as a particle. Rabin and Bibhas obtained a black body spectrum and the corresponding Hawking temperature for a general black hole on a basis of tunneling mechanism with the WKB approximation [35]; Maulik and Frank presented Hawking radiation as a direct tunneling process of particles and derived the tunneling probability as $\Gamma \sim e^{-2\mathrm{Im}S}$, where Im$S$ is the imaginary part of the action for the semi-classical tunneling process [36]. Then they got a standard Hawking temperature formula with a self-gravitation correction [36]. After neglecting the self-gravitation correction, the transmission probability of the particle with energy E satisfies equation (16) [37, 38]:

$$\Gamma \sim \exp\left(-\frac{E}{T_H}\right), \tag{16}$$

where T_H is the Hawking temperature.

In this paper, we use embedding formulas and a projected refractive index to make an optical analogy to Hawking radiation based on the equivalent tunneling picture. We can directly derive the Hawking temperature formula with the particle tunneling probability: $\Gamma \sim e^{-2\mathrm{Im}S}$ [36] in our system (detailed derivations are shown in appendix B).

To check if our optical analogy can exhibit a phenomenon similar to Hawking radiation, we set the parameters as follows: we select equation (12) with $M = 1\ \mu$m and $R = 2.1\ \mu$m, which is close enough to the gravitational radius $r_g = 2\ \mu$m, which means the star is about to collapse to a black hole, and the refractive index of the location of R is 4.58, which is large enough so that the materials can mimic a horizon. As depicted in schematic diagram figure 3(b), we set the gradient of the refractive index on a plane waveguide with 50 μm length and 8 μm width in the x- and y-directions. Region $0 \leqslant r \leqslant 2.1\ \mu$m, corresponds to the inner part of the quasi black hole; region $2.1\ \mu\mathrm{m} \leqslant r \leqslant 50\ \mu$m corresponds to the outside. A beam of plane waves with wavelengths ranging from 0.3 to 0.8 μm and unit amplitude is incident from $x = 0$, propagates along the r-axis, tunnels, and we measure the transmission spectrum at $x = 50\ \mu$m where the index is approximately uniform and equal to one, corresponding to the flat region of Schwarzschild spacetime. In this optical system, the horizon with an infinite refractive index is essentially an infinitely deep barrier, which is the classical problem in quantum mechanics.

We calculate differential equation equation (15) numerically to get the transmission spectrum. The energy E can be expressed as $E = \omega = \frac{2\pi}{\lambda}$. As shown in figure 3(c), we depict the scatter diagram of energy E of particle and natural logarithm of transmission $ln\Gamma$, which shows a linear relationship and the linear coefficient have the same dimension as Schwarzschild radius (where we take $c = k_B = 1$), we express this slope as 2.37 r_g, then we imply that

$$\Gamma \propto \exp\left(-\frac{E}{T_{eff}}\right),$$

with an effective temperature $T_{eff} = 0.422 r_g^{-1}$.

We emphasize that in our analogous system, the surface gravity $\kappa = \frac{1}{4M} = \frac{1}{2r_g}$ is associated with the gravitational radius of the black hole, which is determined by the refractive index distribution along the x-axis. According to equation (12), we can obtain the equation (17):

$$n(x) = \begin{cases} \sqrt{1 + \frac{x^2}{2\kappa \cdot R^3 - x^2}} & 0 < x < R \\ \sqrt{\frac{x}{x - \frac{1}{2\kappa}}} & x \geqslant R \end{cases}. \tag{17}$$

So next we conduct several simulations with a different M in each system. After that we analyze and calculate the corresponding Hawking temperature. We depict data of effective temperatures T_{eff} and surface gravitations κ in figure 3(d), and we find a good linear relationship with a negligible intercept $T_{eff} \propto \kappa$, which is similar to the case in black holes.

4. Conclusion

In conclusion, we have proposed a new method analogous to gravity. It employs an embedding diagram with a projected refractive index for an analogy of cosmological phenomenon such as gravitational collapse and Hawking radiation. We use the variation of the refractive index to simulate the continuous change of the gravitational field of a collapsing star based on a spacetime metric, and we construct an event horizon where the index goes to infinity. Then we observe an analogy to Hawking radiation for the first time. Our method can easily be extended into three-dimensional optical systems to simulate two-dimensional horizons, and in the future we may design and fabricate curved waveguide samples via 3D printing technology, which offers a new experimental approach to simulate Hawking radiation in analogous systems.

Acknowledgments

We thank Yinzhe Ma, Guohua Liang and Runqiu He for their help and helpful comments. Our work was financially supported by the National Natural Science Foundation of China (Nos. 11690033, 61425018, 11621091), National Key R&D Program of China (2017YFA0303702) and National Key Research and Development Program of China (No. 2017YFA0205700). We thank LetPub (www.letpub.com) for its linguistic assistance during the preparation of this manuscript.

Appendix A

In regions of space that contain no free charges and no free currents, we take the curl of the *cual* $-$ $\boldsymbol{E}$ Maxwell equation, interchange the order of space and time derivatives on the right-hand side of the resulting equation, and replace $\nabla \times \boldsymbol{B}$ by $\mu_0\left(\frac{\partial \boldsymbol{D}}{\partial t}\right)$, to obtain the equation

$$\nabla \times \nabla \times \boldsymbol{E} + \mu_0\left(\frac{\partial^2}{\partial t^2}\boldsymbol{D}\right) = 0. \tag{A.1}$$

The first term can be rewritten by vector calculus: $\nabla \times \nabla \times \boldsymbol{E} = \nabla(\nabla \cdot \boldsymbol{E}) - \nabla^2 \boldsymbol{E}$

Then we get the expression:

$$\nabla^2 \boldsymbol{E} - \mu_0 \varepsilon_0 \varepsilon_r \frac{\partial^2}{\partial t^2}\boldsymbol{E} - \nabla(\nabla \cdot \boldsymbol{E}) = 0. \tag{A.2}$$

The third term in equation above has the form:

$$\nabla(\nabla \cdot \boldsymbol{E}) = \nabla\left(\nabla \cdot \frac{\boldsymbol{D}}{\varepsilon(r)}\right) = -\frac{\nabla \varepsilon(r)}{\varepsilon(r)} \cdot \boldsymbol{E}, \tag{A.3}$$

where we use $\nabla \cdot D = 0$ in last step.

Formula (A.2) can be written as:

$$\nabla^2\boldsymbol{E} - \left[\frac{n(r)}{c}\right]^2\frac{\partial^2}{\partial t^2}\boldsymbol{E} + \frac{\nabla\varepsilon(r)}{\varepsilon(r)}\cdot\boldsymbol{E} = 0, \tag{A.4}$$

which is general wave equation in inhomogeneous medium.

Then we express $\boldsymbol{E}(r, t)$ as $\boldsymbol{E}(r, t) = \boldsymbol{E}(r)e^{-i\omega t}$.

The wave equation (A.4) becomes a general Helmholtz equation as:

$$\nabla^2\boldsymbol{E}(r) + [n(r)k_0]^2\frac{\partial^2}{\partial t^2}\boldsymbol{E}(r) + \frac{\nabla\varepsilon(r)}{\varepsilon(r)}\cdot\boldsymbol{E}(r) = 0. \tag{A.5}$$

Especially in our 1D model, the above formula can be simplified as follows:

We assume that electromagnetic wave propagates in the x direction, and relative permittivity ε_r of medium just changes in the x direction, namely $\varepsilon_r = \varepsilon_r(x) = n(x)^2$ the last term vanishes because electric field just have transverse components and gradient term just has longitudinal component:

$$\frac{\nabla\varepsilon(x)}{\varepsilon(x)}\cdot\boldsymbol{E}(y, z) = \frac{1}{\varepsilon(x)} \times \left(\frac{\partial\varepsilon(x)}{\partial x}, 0, 0\right)\cdot(0, E_y, E_z) = 0.$$

Finally, Helmholtz equation (A.5) is represented as:

$$\nabla^2\boldsymbol{E}(x) + [n(x)k_0]^2\frac{\partial^2}{\partial t^2}\boldsymbol{E}(x) = 0. \tag{A.6}$$

Appendix B

The general Schwarzschild black hole metric is expressed as:

$$ds^2 = -f(r)dt^2 + \frac{1}{f(r)}dr^2 + r^2(d\theta^2 + \sin^2\theta d\varphi^2). \tag{B.1}$$

There is only one zero point of $f(x)$ at $r = r_h$ where it is the horizon, and we assume that $f(r) > 0$ for $r > r_h$, corresponding to the exterior of black hole and $f(r) < 0$ for $r < r_h$, corresponding to the interior of black hole. We define surface gravity g_h as:

$$g_h = \frac{1}{2}f'(r_h) > 0. \tag{B.2}$$

We consider this spacetime in our embedding diagram and projected refractive index system, according to equation (11), we obtain index distribution as:

$$n(r) = \sqrt{g_{rr}} = \frac{1}{\sqrt{f(r)}}. \tag{B.3}$$

Then we can define the group velocity v_g of light (in a natural units system with $c = G = k_B = \hbar = 1$) as:

$$v_g = \frac{1}{n(r)} = \sqrt{f(r)}. \tag{B.4}$$

In [36], Parikh *et al* proposed that the imaginary part of action that describes positive energy particle crosses the horizon outwards from the interior of black hole r_{in}, to exterior r_{out} can be expressed as:

$$\mathrm{Im}S = \mathrm{Im}\int_{r_{in}}^{r_{out}} p_r dr, \tag{B.5}$$

where $r_{in} = r_h - \epsilon$, $r_{out} = r_h + \epsilon$, ϵ is infinitesimal.

We consider Hamilton's equation $\dot{r} = \frac{dH}{dp_r}$, where $H = \omega$ and $\dot{r}$ is the equivalent group velocity of light, equal to v_g. We change the variable from momentum to energy and switch the order of integration to obtain:

$$\mathrm{Im}S = \mathrm{Im}\int_{r_{in}}^{r_{out}} p_r dr = \mathrm{Im}\int_0^{\omega}\int_{r_{in}}^{r_{out}}\frac{dr}{v_g}d\omega'. \tag{B.6}$$

We consider equation (B.6) near the event horizon $r = r_h$. Firstly, it is noted that ω' is the frequency of light observed in the infinite, and there is correction factor near the horizon as:

$$\omega' \to \frac{1}{\sqrt{f(r)}}\omega'. \tag{B.7}$$

So equation (B.6) is amended as:

$$\mathrm{Im}S = \mathrm{Im}\int_0^{\omega}\int_{r_{in}}^{r_{out}}\frac{dr}{v_g}d\omega' = \mathrm{Im}\int_0^{\omega}\int_{r_{in}}^{r_{out}}\frac{dr}{f(r)}d\omega'. \tag{B.8}$$

Secondly, we can expand $f(r)$ to second order as:

$$f(r) = f(r)|_{r=r_h} + f'(r)|_{r=r_h}(r - r_h) = 2g_h(r - r_h). \tag{B.9}$$

Substitute equation (B.9) into (B.8), we obtain:

$$\mathrm{Im}S = \mathrm{Im}\int_0^{\omega}\int_{r_{in}}^{r_{out}}\frac{dr}{2g_h(r - r_h)}d\omega'. \tag{B.10}$$

The inner integral is not continuous at the horizon and the two pieces should be connected continuously under the bottom half of complex plane, according to the residue theorem:

$$\int_{r_{in}}^{r_{out}}\frac{1}{2g_h(r - r_h)}dr = \frac{\pi i}{2g_h}. \tag{B.11}$$

So we can obtain equation (B.8) as:

$$\mathrm{Im}S = \mathrm{Im}\int_0^{\omega}\int_{r_{in}}^{r_{out}}\frac{dr}{f(r)}d\omega' = \mathrm{Im}\int_0^{\omega}\frac{\pi i}{2g_h}d\omega' = \frac{\pi\omega}{2g_h}. \tag{B.12}$$

As expressed in [36], the semiclassical tunneling rate has the exponential form:

$$\Gamma \sim e^{-2\mathrm{Im}S} = e^{-\frac{2\pi\omega}{2g_h}} = e^{-\frac{E}{T_H}}, \tag{B.13}$$

where energy $E = \omega$ and temperature $T_H = 2\cdot\frac{g_h}{2\pi}$, which is similar to Hawking temperature formula.

ORCID iDs

Jingming Chen https://orcid.org/0000-0003-2375-246X
Run-Qiu Yang https://orcid.org/0000-0002-5322-0600

References

[1] Abbott B P *et al* 2016 Observation of gravitational waves from a binary black hole merger *Phys. Rev. Lett.* **116** 061102
[2] The Event Horizon Telescope Collaboration 2019 First M87 event horizon telescope results: I. The shadow of the supermassive black hole *Astrophys. J. Lett.* **875** L1
[3] Penrose R 1965 Gravitational collapse and space-time singularities *Phys. Rev. Lett.* **14** 57–9
[4] Hawking S W 1976 Breakdown of predictability in gravitational collapse *Phys. Rev.* D **14** 2460
[5] Hawking S W and Penrose R 1970 The singularities of gravitational collapse and cosmology *Proc. R. Soc.* A **314** 529–48
[6] Sonego S, Almergren J and Abramowicz M A 2000 Optical geometry for gravitational collapse and Hawking radiation *Phys. Rev.* D **62** 064010
[7] Baumgarte T W, Gunalach C and Hilditch D 2019 Critical phenomena in the gravitational collapse of electromagnetic waves *Phys. Rev. Lett.* **123** 171103
[8] Unruh W G 1981 Experimental black-hole evaporation *Phys. Rev. Lett.* **46** 1351–3
[9] Lahav O *et al* 2010 Realization of a sonic black hole analog in a Bose–Einstein condensate *Phys. Rev. Lett.* **105** 240401
[10] Juan R *et al* 2019 Observation of thermal Hawking radiation and its temperature in an analogue black hole *Nature* **569** 688–91
[11] Philbin T G, Kuklewicz C, Robertson S, Hill S, Konig F and Leonhardt U 2008 Fiber-optical analog of the event horizon *Science* **319** 1367–70
[12] Drori J, Rosenberg Y, Bermudez D, Silberberg Y and Leonhardt U 2019 Observation of stimulated Hawking radiation in an optical analogue *Phys. Rev. Lett.* **122** 010404
[13] Cheng Q, Cui T J, Jiang W X and Cai B G 2010 An omnidirectional electromagnetic absorber made of metamaterials *New J. Phys.* **12** 063006
[14] Narimanov E E and Kildishev A V 2009 Optical black hole: broadband omnidirectional light absorber *Appl. Phys. Lett.* **95** 041106
[15] Genov D A, Zhang S and Zhang X 2009 Mimicking celestial mechanics in metamaterials *Nat. Phys.* **5** 687–92
[16] Sheng C, Liu H, Wang Y, Zhu S N and Genov D A 2013 Trapping light by mimicking gravitational lensing *Nat. Photon.* **7** 902–6
[17] Chen Huanyang R X, Miao and Li M 2009 Transformation optics that mimics the system outside a Schwarzschild black hole *Opt. Express* **18** 15183–8
[18] Greenleaf A, Kurylev Y, Lassas M and Uhlmann G 2007 Electromagnetic wormholes and virtual magnetic monopoles from metamaterials *Phys. Rev. Lett.* **99** 183901
[19] Zhu J, Liu Y Q and Jensen L 2018 Elastic waves in curved space: mimicking a wormhole *Phys. Rev. Lett.* **121** 234301
[20] Sheng C, Bekenstein R, Liu H, Zhu S and Segev M 2016 Wavefront shaping through emulated curved space in waveguide settings *Nat. Commun.* **7** 10747
[21] Li M, Miao R X and Pang Y 2010 More studies on metamaterials mimicking de sitter space *Opt. Express* **18** 9026–33
[22] Ginis V, Tassin P, Craps B and Veretennicoff I 2010 Frequency converter implementing an optical analogue of the cosmological redshift *Opt. Express* **18** 5350–5
[23] Sheng C, Liu H, Chen H Y and Zhu S N 2018 Definite photon deflections of topological defects in metasurfaces and symmetry-breaking phase transitions with material loss *Nat. Commun.* **9** 4271
[24] Bekenstein R *et al* 2017 Control of light by curved space in nanophotonic structures *Nat. Photon.* **11** 664–70
[25] Schultheiss V H, Sascha B, Alexander S, Felix D, Stefan N, Andreas T, Stefano L and Ulf P 2010 Optics in curved space *Phys. Rev. Lett.* **105** 143901
[26] Bekenstein R, Kabessa Y, Tal O and Bandress M 2015 Observing light dynamics in micro-sized Schwarzschild metric *Lasers Electro-Optics* (Piscataway, NJ: IEEE) (https://doi.org/10.1363/CLEO_QELS.2015.FTu4C.2)
[27] Agranat A *et al* 2016 Curved space nanophotonics inspired by general relativity *Lasers Electro-Optics* (Piscataway, NJ: IEEE) (https://doi.org/10.1364/CLEO_QELS.2016.FW1D.2)
[28] Marolf D 1999 Spacetime embedding diagrams for black holes *Gen. Relativ. Gravit.* **31** 919–44
[29] Hledik S, Stuchlik Z and Cipko A 2006 Visualizing spacetimes via embedding diagrams *AIP Conf. Proc.* (https://doi.org/10.1063/1.2399673)
[30] Jr J T G, Marolf D and Garvey R H 2003 Spacetime embedding diagrams for spherically symmetric black holes *Gen. Relativ. Gravit.* **36** 83–99
[31] Oppenheimer J R and Snyder H 1939 On continued gravitational contraction *Phys. Rev.* **56** 455–9
[32] Oppenheimer J R and Volkoff G M 1939 On massive neutron cores *Phys. Rev.* **55** 374–81
[33] Hawking S W 1975 Particle creation by black holes *Commun. Math. Phys.* **43** 199–220
[34] Hawking S W 1974 Black hole explosions? *Nature* **248** 30–1
[35] Banerjee R and Majhi B R 2009 Hawking black body spectrum from tunneling mechanism *Phys. Lett.* B **675** 243–5
[36] Parikh M K and Wilczek F 2000 Hawking radiation as tunneling *Phys. Rev. Lett.* **85** 5042–5
[37] Hartle J B and Hawking S W 1976 Path-integral derivation of black-hole radiance *Phys. Rev.* D **13** 2188–203
[38] Ren J R, Ran L I and Liu F H 2009 Hawking temperature of dilaton black holes from tunneling *Mod. Phys. Lett.* A **23** 3419–29